

Magnetic-impurity oscillations and the low-temperature photokinetics in germanium

V. F. Gantmakher and V. N. Zverev

Institute of Solid State Physics, USSR Academy of Sciences

(Submitted November 26, 1975)

Zh. Eksp. Teor. Fiz. 70, 1891-1906 (May 1976)

The magnetic-impurity oscillations previously observed by the authors in germanium {Zh. Eksp. Teor. Fiz. 69, 695 (1975) [Sov. Phys. JETP 42, 352 (1976)]} are investigated. The suggestion that the oscillations are due to inelastic scattering of electrons by neutral acceptors is confirmed by experiments on germanium doped with indium, or on germanium with various gallium impurity concentrations N_A between 5×10^{13} and 10^{15} cm^{-3} . The oscillations disappear abruptly when the concentration N_A is increased from 10^{15} to $3 \times 10^{15} \text{ cm}^{-3}$. An explanation is attempted by assuming the existence of comparatively long-lived excited states of acceptors that migrate along the crystal. Some experimental facts concerning the photokinetics of the oscillations are observed. Thus, the potential difference between the illuminated and nonilluminated sides of the sample is found to oscillate simultaneously with the photomagnetic field E_{GH} ; there is a peak in the dependence of E_{GH} on the light intensity in the oscillation inversion region, if the magnetic field H is constant; if H lies in the plane of the sample, then the depth distribution of the carriers is determined by the hot carriers and depends on the frequency of the interband irradiation; infrared irradiation alters the oscillation pattern radically. A number of features of the kinetic problem under consideration are formulated on the basis of these facts. These are the absence of a background of equilibrium carriers, the distinctive role of the hot electrons, some peculiarities of the depth distribution of the carriers, and peculiarities of scattering of electrons by phonons at helium temperatures.

PACS numbers: 72.15.Qm, 72.40.+w

INTRODUCTION

An investigation of the galvanomagnetic characteristics of *p*-germanium subjected to interband photoexcitation at helium temperatures^[1] has revealed oscillations periodic in the reciprocal magnetic field. Oscillations of this type are usually described by the relation

$$(\mathcal{N} + \gamma) \hbar \Omega = \mathcal{E} \quad (\Omega = eH/mc; \mathcal{N} = 1, 2, 3, \dots; |\gamma| < 1), \quad (1)$$

where \mathcal{E} is a certain energy, m and e are the effective mass and charge of the electron, and H is the magnetic field. It was shown in^[1] that in this case the expression for the oscillation period

$$P = \Delta(1/H) = \hbar e / mc \mathcal{E}, \quad (2)$$

which follows from (1), contains the cyclotron mass m of the electrons in the conduction band (at $H \parallel [100]$, $m = 0.135m_0$), and the energy \mathcal{E} is equal to the difference between the energies of the ground state and the lowest excited state of the neutral acceptor. This means that the kinetic parameters of the system are strongly influenced by the oscillations of the probability of inelastic scattering of the electrons by the neutral acceptors.

Oscillations of the scattering probability were discussed many times as applied to magnetophonon resonance (see, e.g.,^[2,3]). They are connected with the fact that in a magnetic field the density of states of the electrons in the band has a singularity near the bottom of each Landau subband. When condition (1) is satisfied, the number of transitions for which there are singularities in the density of both the initial and final states increases. As a result, the average transition frequency also increases. In the experiments discussed below, the nature of the scattering-probability oscillations is the same, but scattering process itself is dif-

ferent. Instead of emission or absorption of optical phonons, transitions take place between states of the neutral acceptor. Resonant inelastic scattering by impurities was observed also in^[4].

On the whole, the entire problem of magnetic-impurity oscillations breaks up in natural fashion into two parts. The first deals with the energy relations that govern the oscillations. The second concerns the kinetics of the photoelectron gas in which the inelastic-scattering processes take place. Our earlier paper^[1] was devoted mainly to questions of the first type. We ascertained which factors do or do not influence the period of the oscillations and explained the physical meaning of the quantity \mathcal{E} contained in (1) and (2). In passing, however, we observed a number of purely kinetic phenomena, namely, strong dependences on the temperature and on the inversion of the oscillations. In this paper we also touch upon both groups of questions and consequently the entire material is broken into two parts. The stress, however, is now on questions dealing with the kinetics of the photomagnetic effect.

PROCEDURE

The measurement procedure employed is described in detail in^[1]. Just as before, the experiments were performed in two configurations, with the magnetic field H along the normal to the surface (vector $H \parallel z$ in Fig. 1; we call this the case of longitudinal-diffusion configuration, since the carriers produced at the surface diffuse along the field H), and with the field H in the plane of the surface (vector $H \parallel x$ or $H \parallel y$; transverse-diffusion configuration). With the field direction $H \parallel y$ we measured the photomagnetic-effect, electric field E_{GH} which is perpendicular to the field H and to the density gradient and is produced when a light flux G is incident on the surface. At $H \parallel x$ we measured the

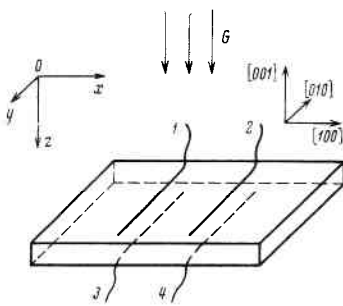


FIG. 1. Placement of contacts on the sample; G —light flux incident on the sample.

longitudinal magnetoresistance. In all three cases, H was directed along the same crystallographic axis $\langle 100 \rangle$.

The samples measured approximately $4 \times 4 \times 0.2$ mm. In addition to the two contacts used in ^[1] (contacts 1 and 2 in Fig. 1), two other contacts (3 and 4) were attached to the dark side of some of the samples. They made it possible to measure the potential difference between the illuminated and the dark surfaces in both configurations, and also to check on the effect of the illumination of the contacts on the performed measurements. The distance between contacts was ~ 1 mm.

The carriers were excited with a 10-mW He-Ne laser. Lasing at a wavelength 0.63μ was used in most experiments. However, by switching the mirror without changing the beam geometry the laser could be retuned to a wavelength 1.15μ . The illuminated region, in the form of a spot of 3 mm diameter, overlapped the gap between the contacts. To increase the illumination intensity, the spot could be focused with a cylindrical lens into a strip of $\sim 100 \mu$. The illumination intensity I will be expressed throughout in terms of the number of photons incident per second on a unit surface of the sample. The maximum intensity in ^[1] corresponded to $(2-3) \times 10^{18}$ $\text{cm}^{-2} \text{sec}^{-1}$.

ELEMENTARY INELASTIC SCATTERING PROCESS

Our earlier conclusions ^[1] concerning the causes of the oscillations and concerning the physical meaning of \mathcal{E} were based, besides the agreement with the values of the corresponding energies obtained from spectroscopic measurements, ^[5,6] only on one direct experiment, namely on the change of the period when the principal doping impurity was changed. Since this conclusion is of fundamental significance for our prob-

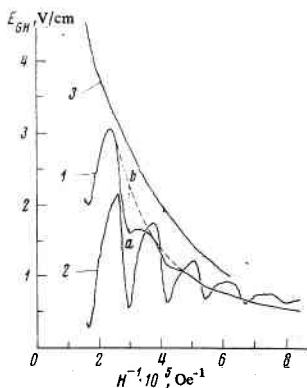


FIG. 2. Oscillations of the field E_{GH} on 3- Ω (curve 1, $T = 2.14^\circ\text{K}$) and 40- Ω (curve 2, $T = 1.31^\circ\text{K}$) germanium samples. In both bases $I \approx 10^{17} \text{ cm}^{-2} \text{ sec}^{-1}$, ab is the depth of the second minimum, arbitrarily assumed henceforth to be the amplitude A of the oscillations. Curve 3—plot of $E_{GH}(H^{-1})$ for 1- Ω germanium ($T = 2.2^\circ\text{K}$, $I \approx 10^{17} \text{ cm}^{-2} \text{ sec}^{-1}$).

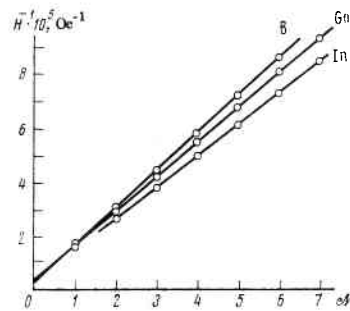


FIG. 3. Dependence of the position of the extrema of the oscillations on the number N for different doping impurities.

lem, several additional experiments were performed.

We investigated first, a series of samples with one doping impurity (gallium) but with different concentrations. We used commercial germanium with seven different values of the room-temperature resistivity ρ in the interval from 40 to 1 $\Omega\text{-cm}$. It was assumed that ρ determines uniquely the acceptor density N_A , and the agreement was established on the basis of a graph given in Shalyt's review. ^[7] The presence of oscillations was verified by measuring the dependence of the field E_{GH} on H . It appears that these measurements are more sensitive to the oscillations than measurements of the photoconductivity in the longitudinal-diffusion configuration. ^[8]

The oscillations were observed at all doping levels in the indicated interval, with the exception of the maximum level ($\rho = 1 \Omega\text{-cm}$, $N_A = 3 \times 10^{15} \text{ cm}^{-3}$). The period of the oscillations was independent of ρ —see Fig. 2. We were unable to observe the oscillations in the germanium samples with resistivity 1 $\Omega\text{-cm}$. It can be stated that if there are any oscillations of E_{GH} at all in these samples, they amount to not more than 1–2% of the monotonic part of the signal, and are therefore difficult to register in our measurement procedures. For the samples with N_A only one-third as large ($\rho = 3 \Omega\text{-cm}$), however, the oscillation amplitude amounted in individual cases to as much as 30% of the monotonic part of the signal (Fig. 2). We shall return to a discussion of this fact later on.

Second, in addition to the earlier measurements ^[1] of the oscillations $E_{GH}(H^{-1})$ in germanium doped with gallium and boron, we performed similar measurements on samples doped with indium ($N_A = 1.4 \times 10^{14} \text{ cm}^{-3}$). Figure 3 shows the dependence of the position of the extrema of the oscillations, in the form of a plot of $1/H$ against the number N for three different acceptor impurities in germanium. The values of the energy \mathcal{E} determined for all three impurities from the slopes of the lines in Fig. 3 in accordance with formula (2) agreed with good accuracy with the difference $\Delta\mathcal{E}$ between the energies of the ground and first excited states of the corresponding acceptor in germanium, as measured spectroscopically by Jones and Fisher ^[5] (see Table 1). As noted in ^[1], allowance for the dependence of the energy spectrum of the acceptor on the magnetic field changes the energies \mathcal{E} insignificantly.

There is no doubt that the quantities in the last two columns of Table 1 are correlated. It remains unclear, however, which of the two elementary inelastic-

TABLE 1.

Impurities	$P \cdot 10^3, \text{Oe}^{-1}$	ϵ, meV	$\Delta \epsilon, \text{meV}[\%]$
In	1.15 ± 0.03	7.5 ₀	7.39 ± 0.01
Ga	1.25 ± 0.02	6.8 ₀	6.74 ± 0.01
B	1.37 ± 0.03	6.2 ₀	6.24 ± 0.01

scattering processes is decisive, the downward energy transition of the energy by $\mathcal{N}\hbar\Omega$ with excitation of an acceptor, or the increase of the energy of the cold electron by $\mathcal{N}\hbar\Omega$ as a result of the transition of the excited acceptor to the ground state.

In^[1] we presented the following two arguments favoring the second process: the strong temperature dependences, which indicate that the principal role in the kinetics of the oscillations is indeed played by the cold carriers, and the absence of a fine structure of the oscillations, meaning that the transition with participation of the lowest excited state is distinguished from the other transitions. Yet note was taken there also of the difficulty encountered by the assumption that scattering of cold carriers by excited acceptors plays the predominant role, inasmuch as this calls for the lifetime τ^* of the acceptor in the excited state to be

$$\tau^* \geq 10^{-6} \text{ sec.} \quad (3)$$

There are discrepancies between this inequality and the theoretical estimate.^[9] These discrepancies, however, are not so large, especially in light of later numerical calculations.^[10] The calculations in^[9,10], however, were made for donors, and until analogous calculations are available for acceptors it can hardly make sense to discuss these discrepancies in detail.

At the same time, the large time τ^* in conjunction with the already mentioned vanishing of the oscillations at $N_A \geq 3 \times 10^{15} \text{ cm}^{-3}$ admits, in our opinion, of one more argument favoring the second process. Indeed, at $N_A \approx 10^{15} \text{ cm}^{-3}$ overlap of the wave functions of the excited state and the smearing of the corresponding levels can come into play. According to measurements by Colbow^[11] on silicon at $N_A = 1.2 \times 10^{16} \text{ cm}^{-3}$, the broadening of the lower excited states of the acceptors is $\delta \epsilon \approx 0.7 \text{ meV}$. On the basis of the fact that the relative broadening $\delta \epsilon / \epsilon_0$ depends on the dimensionless parameter $N_A^{-1/3} / a \sim N_A^{-1/3} \kappa \epsilon_0$ ($a = e^2 / 2\kappa \epsilon_0$ is the effective Bohr radius, κ is the dielectric constant, and ϵ_0 is the acceptor ionization energy) we find for germanium with $N_A \approx 4 \times 10^{14} \text{ cm}^{-3}$ a broadening $\delta \epsilon \approx 0.2 \text{ meV}$.

This broadening is not large enough to influence the electron-phonon interaction or the probability of elec-

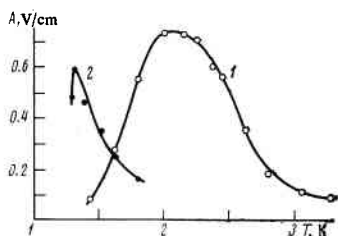


FIG. 4. Oscillation amplitudes A (see the caption of Fig. 2) as a function of T . Curve 1— $\rho = 5 \text{ } \Omega\text{-cm}$, $I \approx 10^{16} \text{ cm}^{-2} \text{ sec}^{-1}$, 2— $\rho = 40 \text{ } \Omega\text{-cm}$, $I \approx 10^{17} \text{ cm}^{-2} \text{ sec}^{-1}$.

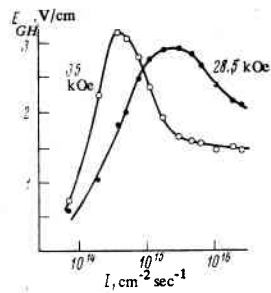


FIG. 5. Dependence of $E_{GH}(I)$ at two values of the magnetic field; $\rho = 30 \text{ } \Omega\text{-cm}$, $T = 1.5 \text{ } ^\circ\text{K}$.

tron transitions to lower energies with excitation of acceptors. Yet this broadening means that the time of the transition of the excitation to the neighboring acceptor is of the order of $\tau^{**} \approx \hbar / \delta \epsilon \approx 3 \cdot 10^{-12} \text{ sec}$. With further increase of N_A , the broadening connected with the overlap of the wave functions increases exponentially. The excited state begins to migrate over the acceptors in analogy with an electron migrating over the impurities in hopping-conductor processes,^[12] or similar to a molecular exciton. Sooner or later this excitation will land on some recombination center and vanish. It is known that there is a concentration threshold for such a migration—percolation. It appears that at $N_A \approx 3 \times 10^{15} \text{ cm}^{-3}$ in germanium the migration loss already limits τ^* and leads to violation of the inequality (3).

PHOTOKINETICS: RESULTS

In this section we attempt to gather and systematize the most important experimental facts pertaining to photokinetics. For convenience in the discussion that follows we break up the material in several sections.

1. One of the most important experimental facts is that the photocurrent, the field E_{GH} , the oscillation amplitude, etc. depend strongly on the amplitude, as does also in a number of cases the inversion of the oscillations at helium temperatures. Several examples of this dependence have already been given in^[1]. The temperature interval in which oscillations could be observed depended on the acceptor concentration N_A . This dependence was investigated in greater detail by observing the oscillations of the photomagnetic effect. With increasing N_A , the interval in which the oscillations were observed shifted towards higher temperatures (see Fig. 4). In samples with large amplitude of the oscillations of E_{GH} it was possible to choose the excitation level I such that a change of T produced inversion; a typical series of such plots is shown in Fig. 10 of^[1]. This was easiest to do at medium values of N_A ($\rho = 10, 15, \text{ and } 30 \text{ } \Omega\text{-cm}$, $N_A = 3, 2, \text{ and } 0.7 \times 10^{14} \text{ cm}^{-3}$). On samples with $\rho = 40 \text{ } \Omega\text{-cm}$ and $N_A = 0.5 \times 10^{14} \text{ cm}^{-3}$, inversion of the oscillations of E_{GH} was observed only in individual experiments, while for the samples with the remaining concentrations ($\rho = 3 \text{ and } 5 \text{ } \Omega\text{-cm}$, $N_A = 10 \text{ and } 6 \times 10^{14} \text{ cm}^{-3}$) the inversion was not observed at all, (see, however, Sec. 8 below).

2. At a fixed magnetic field, however, we were able to measure the dependence of $E_{GH}(I)$ on the illumination intensity I or on the temperature T . Figure 5 shows the measured $E_{GH}(I)$ for a sample of 30- Ω germanium

at two values of the magnetic field: in a resonant field of 35 kOe, corresponding to $\lambda^0 = 2$, and in a nonresonant field of 28 kOe. Attention is called to the presence of maxima on these curves. Similar $E_{GH}(I)$ curves were obtained also for the samples of 15- and 10- Ω germanium, the intersection point of the curves in the resonant and nonresonant fields, which can be called the point of oscillation inversion, was always between the maxima.

The intensity I at which E_{GH} has a maximum depends on T . This dependence is shown in Fig. 6 for the same two values of the magnetic field as in the preceding figure. These curves divide the (I, T) plane into two regions. In the first (region I) the resonances take the form of deep minima, and in the second (region II) they are maxima. These regions are separated by a strip in which the inversion of the E_{GH} oscillations takes place.

We note that once the presence of the maximum on the $E_{GH}(I)$ curve and the shift of this curve to the left at resonance are explained, the oscillation inversion also becomes immediately understandable. Therefore the functions plotted in Figs. 5 and 6 can be crucial for the explanation of the high-temperature kinetics under transverse diffusion conditions.

The maximum of the $E_{GH}(I)$ curves for the 40- Ω , 3- Ω , and 5- Ω germanium usually occurred at intensities for which the oscillations have already practically vanished. It was noted in general that to observe oscillations in these samples the required intensities were larger by approximately one order of magnitude than for samples with medium values of N_A .

3. As already noted,^[1] the frequency of the interband irradiation exerts no influence whatever on the photoconductivity curves in the longitudinal-diffusion configuration. At the same time, in the case of transverse diffusion the decrease of the photon energy from 1.96 to 1.08 eV (changeover to the wavelength 1.15 μ) greatly decreased the field E_{GH} , so that the corresponding potential difference became comparable with the parasitic photo-emf between the contacts. Under these conditions the oscillations became less pronounced, but their period remained the same as before.

To estimate the inhomogeneity in the distribution of the photocarriers over the sample thickness, we could

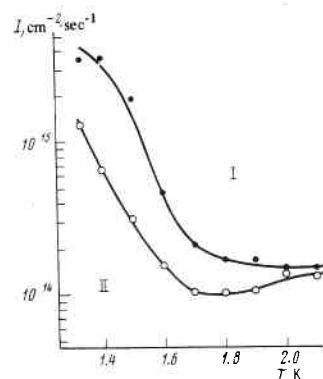


FIG. 6. Position of the maximum on the $E_{GH}(I)$ and temperature dependence at $H = 35$ kOe (lower curve) and $H = 28.5$ kOe (upper curve), $\rho = 30 \Omega\text{-cm}$.

use the ratio of the resistances between contacts 1 and 2 and contacts 3 and 4 in a constant magnetic field H perpendicular to the measuring current. In longitudinal diffusion, the ratio R_{12}/R_{34} of these resistances was ~ 0.95 at both wavelengths at a sample thickness $d = 0.12$ mm in a field $H = 21$ kOe. At the same d and H , but under transverse-diffusion conditions, the ratio R_{12}/R_{34} was ~ 0.35 and ~ 0.05 when exposed to the wavelengths 0.63 and 1.15 μ , respectively.

4. We proceed now to an exposition of the results of the measurements of the potential difference U between the illuminated and non-illuminated sample surfaces. It consists generally of the potential difference

$$U_D = \int_0^d E_D(H, z) dz$$

due to the electric field in the sample volume (the Demmer field) and the contact photo-emf. The latter depend on T as well as on H and on I . They could be excluded in the measurements of the field E_{GH} by varying the direction of the magnetic field, inasmuch as the contact emf do not depend, in first-order approximation, on the field direction, while E_{GH} is replaced by $-E_{GH}$. This cannot be done in measurements of U . Nevertheless, we still assume that in most cases the change of the field E_D in the volume of the crystal made the principal contribution to U , and attempt subsequently to justify this assumption.

In a zero magnetic field, the value of U was less than 5 mV. This means that the upper limit of U_D is also of the same order. Application of a magnetic field perpendicular to the surface (longitudinal diffusion) produced a potential difference $U^{(1)}$ that increased with increasing field. It was different in magnitude for different pairs of contacts, reaching 50–100 mV in a field of 50 kOe. The positive terminal was always on the non-illuminated surface. If it is assumed that $U^{(1)}$ is determined principally by the volume field E_D , then this sign of the potential difference points to a faster diffusion of the holes.

In general, oscillations were observed on the $U^{(1)}(H)$ plot, but of very small amplitude, on the order of 5 mV for some pairs of contacts and not more than 1 mV for others. There was no assurance whatever that these oscillations were not due to extraneous circumstances (inaccurate placement of the contacts over each other, deviation of the magnetic field from normal to the surface, etc.).

5. Under transverse-diffusion conditions, U had predominantly an "electronic" sign (positive on the illuminated surface) and underwent very strong magnetic-impurity oscillations (Figs. 7 and 8). Since the scattering mechanism causing the oscillations is of volume origin, it is natural to assume that the amplitude of the oscillations is determined entirely by the change of the field E_D in the volume of the sample.

The absolute values of the oscillation amplitude, which characterizes U_D turn out to be approximately the same as the values of the photomagnetic potential

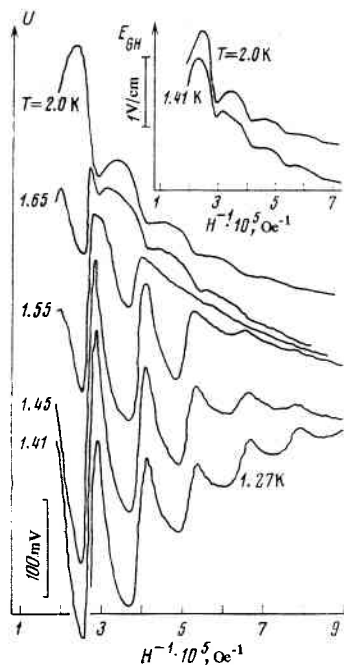


FIG. 7. Oscillations of the potential difference U at different temperatures of a sample of 15- Ω germanium; $I = 5 \times 10^{15} \text{ cm}^{-2} \text{ sec}^{-1}$. Inset—oscillations of E_{GH} recorded in the same experiment.

difference. The sample thickness d , however, is one fifth as large as the distance between the contacts; furthermore, the modulation depth, as we have seen, is smaller than d in the case of transverse diffusion. This means that the field E_D reaches in some cases (e.g., under the conditions of the $T = 1.41 \text{ }^\circ\text{K}$ curve in Fig. 7) a tremendous value, 50–100 V/cm. We point out by way of comparison that low-temperature breakdown in a transverse 40-kOe magnetic field occurs at an electric field intensity not larger than 30 V/cm (see also Fig. 7 of [1]).

6. It is seen from Figs. 7 and 8, which shows simultaneously measured plots of $U(H^{-1})$ and $E_{GH}(H^{-1})$, that in the (I, T) plane neither the regions of the maximum amplitude of the oscillations of E_{GH} and U nor the places where the oscillations of these quantities undergo inversion, are in agreement. As shown in Sec. 3, under transverse-diffusion conditions the carriers are unevenly distributed over the sample thickness. It is probable that the principal role in the formation of the field E_{GH} is played by surface layers with maximum carrier density; on the other hand, when the potential difference U_D is formed, the deeper carrier-poor layers cannot be significant. This explains, for example, the presence of tremendous oscillations of U at $T = 1.27 \text{ }^\circ\text{K}$ at the same time that there are no oscillations of E_{GH} (curves 1 in Fig. 8).

We recall in this connection that inversions of the oscillations of the magnetoresistance and of the oscillations E_{GH} also took place at different intensities. [1] It is quite possible, however, that owing to the difference in the diffusion conditions the inversion took place in both cases at approximately the same average carrier densities.

7. Several measurements of the photoconductivity were made at a field direction $\mathbf{H} \parallel \mathbf{x}$ and a measuring current $\mathbf{j} \parallel \mathbf{H}$. (The parallelism of the field direction to

the sample surface can be easily set by means of the resistance minimum: a 3° deviation of the field from the surface doubles the resistance.) In a 50-kOe field, the sample resistance increased by several dozen times in comparison with the resistance in a zero field. Oscillations on the $j(H)$ curve were observed in not all the experiments, and their relative amplitude sometimes did not exceed 10%. Just as in the measurement of $U^{(1)}(H)$ (see Sec. 4), the appearance of weak oscillations of j in the presence of strong oscillations of other kinetic parameters (U_D and the transverse magnetoresistance) can be due to the fact that they are not sufficiently well decoupled in the experiment. In particular, even though in this experiment we measured the longitudinal magnetoresistance, the carrier distribution $n(z)$ was governed all the same by the transverse diffusion process.

8. In all the experiments described above, the light beam incident on the sample passed through a glass plate located in the liquid helium. This plate filtered out the thermal radiation. Without it the sample was exposed to weak infrared radiation that ionized the acceptors partially. The oscillation picture was then strongly altered. The oscillations decreased in amplitude and vanished when the interband illumination intensity I was larger by approximately one order of magnitude; inversion of the oscillations of E_{GH} set in for the samples of 40- Ω and 5- Ω germanium.

PHOTOKINETICS: DISCUSSION

The equilibrium carrier densities n_0 and p_0 in germanium are so low at helium temperatures that in our experiments the photoelectron and photohole densities n and p always satisfied the inequality

$$n, p \gg n_0, p_0. \quad (4)$$

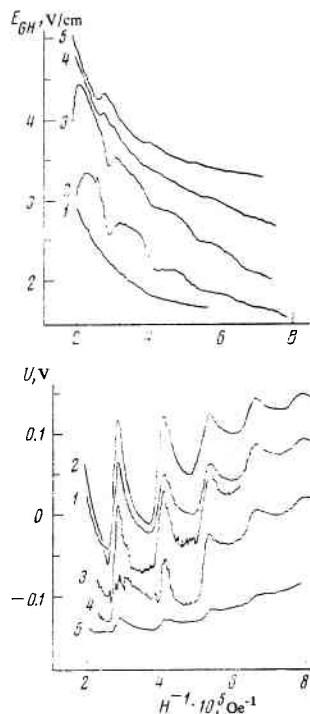


FIG. 8. Oscillations of U and E_{GH} recorded in a single experiment: $T = 1.27 \text{ }^\circ\text{K}$, $\rho = 15 \text{ } \Omega\text{-cm}$. Intensities $I [\text{cm}^{-2} \text{ sec}^{-1}]$: 1- 10^{17} , 2- $2 \cdot 10^{16}$, 3- $2 \cdot 10^{15}$, 4- $7 \cdot 10^{14}$, 5- $2 \cdot 10^{14}$.

TABLE 2.

Group No.	$\bar{\epsilon}$, K	v , cm/sec	R , cm	τ , sec	t , sec	L , cm
1	5000	10^8	10^{-4}	10^{-12}	$10^{-11}-10^{-10}$	10^{-3}
2	100	10^7	10^{-5}	10^{-10}	10^{-8}	10^{-4}
3	2	10^6	10^{-6}	10^{-9}	$10^{-4}-10^{-6}$	10^{-5}

This means that we have encountered a different limiting case in comparison with that which occurred in low-temperature experiments on InSb^[6,13] and was considered in a number of theoretical papers.^[13,14]

The first and simplest consequence of the inequality (4) was the relatively large intensity of the electric field E , produced in the volume of the crystal in the course of the diffusion. Indeed, the field E was determined by the condition that the current $j^{(E)} \sim (n+n_0)\mu E$ produced under the influence of this field must cancel out the diffusion current $j^{(d)} \sim e\nabla nD$ (μ is the mobility and D is the diffusion coefficient). If $n \ll n_0$, then E contains a small factor n/n_0 but when the inequality (4) is satisfied there is no such factor. Therefore, for example, in our experiments the field E_{GH} was of the order of volts and not millivolts as is usual in germanium.^[15] The Dember field should also be much larger than usual, and this served as one more argument that the measured quantity U (see Secs. 4 and 5 above and Figs. 7 and 8) are determined mainly by the field in the interior of the sample.

According to Sec. 3, in the transverse-diffusion configuration, the strong temperature dependences can be simultaneously accompanied by an influence of the illumination frequency on the photomagnetic effect. Consequently, an important role in the kinetics is played in this case by both the thermalized and non-thermalized carriers.

We divide all the electrons into three groups: 1) hot electrons with energies ϵ from the electron-production energy ~ 1 eV to the optical phonon energy $\hbar\omega_0 = 37$ meV, which are cooled by emission of optical phonons; 2) warm electrons with in the interval $\hbar\omega_0 > \epsilon > kT$, which are cooled mainly by emission of acoustic phonons; 3) cold electrons with the bath temperature T and surviving until they are bound into excitons. The tentative values of the average energy $\bar{\epsilon}$, of the velocity v , of the Larmor radius R , of the momentum relaxation time τ , of the lifetime t in the given group, and of the diffusion length $L = R\sqrt{t/\tau}$ are listed in Table 2 for the electrons of these three groups. The ratio of the number of electrons in these groups is $n_1 : n_2 : n_3 = t_1 : t_2 : t_3$.

The first three columns of the table need no comment. The times τ_1 and τ_2 are governed by the phonon emission probability and the time τ_3 by the probability of scattering by neutral acceptors. The lifetime is $t_1 = g\tau_1$, where g is the number of emitted optical phonons and is determined by the initial energy of the produced electrons. Assuming that approximately half of the excess photon energy is converted into kinetic energy of the electron, we find that at an interband excitation wavelength 0.63μ we obtain $g \approx 20$, as against $g \approx 5$ for 1.15μ . The diffusion length $L_1 \approx R_1 g^{1/2}$ changes cor-

respondingly. The value of t_3 is calculated under the assumption that the main channel whereby the cold carriers are removed is binding into excitons. Strictly speaking, however, there are no experimental data that justify this assumption, since the quantum yield in all the experiments on recombination luminescence is of the order of 1%.

In the calculation of τ_i in the table no account was taken of the electron-electron collisions. If we use for the frequency of the electron-electron collisions in a zero magnetic field the tentative formula

$$\tau_{ee}^{-1} \approx ne^4/\kappa^2 m^{3/2} \bar{\epsilon}^3, \quad (5)$$

then we obtain $\tau_{ee} \gg \tau_{1,2}$ for the hot and warm electrons and $\tau_{ee}^{(3)} \approx 10^{-9}$ sec $\approx \tau_3$ for the cold ones. To be sure, since $\hbar\Omega \gg kT$ and all the cold electrons are on the same Landau level, electron pair collisions should not contribute to the scattering. It seems, however, that these collisions take place in most cases in the field of immobile scattering centers, so that formula (5) is valid for estimates also in a strong magnetic field.^[16]

It is seen from the last column of the table that the diffusion electron flux along the z axis consists mainly of hot and thermal electrons; owing to the small R_3 , cold electrons do not take part in the diffusion. This explains the influence of the frequency of the interband illumination (Sec. 3). The electrons produced by low-energy photons cool down too rapidly to be able to diffuse into the interior, so that the entire distribution is crowded towards the surface.

Thus, in experiments with transverse diffusion the initial diffusion current along the z axis and the scale of the distribution over the depth are governed by the hot carriers. The diffusion current along the x axis

$$j_x^{(d)} \approx \frac{c}{H} \sum \nabla n_i \bar{\epsilon}_i \quad (6)$$

can be produced by all the groups, but since $\Omega\tau_3 \gg 1$, it is not influenced by the scattering of the cold electrons and it can depend on T only via ∇n_3 . To explain the role of the temperature (Sec. 1) it becomes therefore necessary to assume that the field currents $j_x^{(E)}$ and $j_z^{(E)}$ that compensate for the diffusion are determined by the cold electrons. Since the contribution made to the diffusion by a given electron group is determined by the quantity D_i , while their contribution to $j^{(E)}$ is determined by μ_i , and since $D_i = \bar{\epsilon}_i \mu_i / e$, this "distribution of the obligations" takes the form of the inequalities

$$1 \ll D_i / D_3 \ll \bar{\epsilon}_i / kT. \quad (7)$$

In the case of longitudinal diffusion, when $L \approx v\sqrt{t\tau}$, it seems that the hot electrons take no part at all in the kinetics. Therefore the change of the pump wavelength is not reflected at all in the value of the current and in the shape of the photoconductivity curves. The increase of the Dember field when a field $H \parallel z$ is turned on, and the sign of this field, are also easily explained without invoking hot electrons. It is known that the longitudinal mobility of the electrons in germanium at $H \parallel [100]$ is one-fifth their mobility in a zero field, because the principal axes of the electron ellipsoids, corresponding

to a large mass, make an approximate angle 55° with the [100] axis. Naturally, a decrease of the electron mobility is accompanied by an increase of the field E_D with "hole sign," stimulating electron flow into the interior of the sample.

It must be emphasized that under the conditions of transverse diffusion the distribution of the hot and cold electrons along the z coordinate is different. Assume that, just as in the case of electrons, there are hot and cold holes and that all the hole parameters are the same as for the electrons. Then the diffusion of the hot carriers is not accompanied by the appearance of an electric field along the z axis and their distribution is given by $n_1(z) = p_1(z) \propto \exp(-z/L_1)$. The distribution of the cold carriers produced upon cooling of the hot carriers which practically do not diffuse and vanish by binding into electrons, i. e., on account of quadratic recombination, is determined by the ratio $n_1(z)/t_1 = \kappa_{ex} n_3^2(z)$ (κ_{ex} is the kinetic binding coefficient). Hence $n_3 \propto \exp(-z/2L_1)$.

We note that a distribution of a very different type is obtained if we forgo the distinction between the hot and cold carriers and assume that their kinetic parameters remain unchanged during their lifetime. In this limiting case, owing to the quadratic character of the recombination, the distribution is given by the function $n(z) \propto (z+C)^{-2}$, where C is a constant determined from the boundary conditions. It is seen therefore that any imbalance in the parameters of the hot groups of electrons and holes, e. g., a difference in the times t_1 , causes the distributions $n_1(z)$ and $n_3(z)$ to be proportional not to exponentials but to more complicated functions.

Even greater complications arise in the question of the carrier distribution at those values of z at which the Debye radius becomes larger than the characteristic scale of the change of the concentration along the z axis. This region of z seems to occur far from the illuminated surface.

Attempts to explain many of the experimental facts described above, such as the dependence of the temperature interval in which the oscillations are observed on the impurity concentration (Sec. 1), the presence of a maximum of E_{GH} when the intensity I is varied (Sec. 2), the presence of inversion of the oscillations (Secs. 5 and 6), up against the question of the relation between the different mechanisms of scattering and recombination of cold carriers. The material in Secs. 2 and 6 attests to the influence exerted on the inversion of the oscillations by the carrier density. This means that an important role is played by electron-electron collisions and by quadratic recombinations. The oscillations themselves are due to scattering by impurities, and besides the inelastic scattering there is also elastic scattering. The processes involving outflow of energy from the electron system depend essentially on the electron-phonon scattering. The complicated dependences of the probabilities of all these processes confuse the entire picture.

The central problem in this group, in our opinion, is the temperature dependence. Usually the probabilities

of all scattering processes are given by relatively slow power-law functions of the temperature. It is therefore surprising that a change of only 0.2°K (15%) in the temperature can produce such dramatic changes as in the plots of Fig. 7 (see also Fig. 10 of^[11]). In this connection, we wish to call attention to some features of electron-phonon interaction in this temperature region.

The electron spectrum of germanium in a magnetic field is given by

$$\varepsilon = \mathcal{N} \hbar e H / mc + p^2 / 2m^*, \quad (8)$$

where^[17]

$$m = \left(\frac{m_1 m_2^2}{m_1 \cos^2 \varphi + m_2 \sin^2 \varphi} \right)^{1/2}, \quad m^* = \frac{m_1^2 \cos^2 \varphi + m_2^2 \sin^2 \varphi}{m_1 \cos^2 \varphi + m_2 \sin^2 \varphi} \quad (9)$$

($m_1 = 1.58m_0$ and $m_2 = 0.082m_0$ are the principal values of the effective-mass tensor, φ is the angle between the vector H and the [111] axis). It is seen from (9) that even at relatively large angles φ the cyclotron mass, which determines the distance between the Landau subbands remains small and close to m_2 , while the mass m^* , which describes the motion in the interior of each band is large and close to m_1 . At $H \parallel [100]$ ($\varphi = 55^\circ$), when all the electron valleys are equivalent, we have $m = 0.135m_0$ and $m^* = 1.43m_0$. Thus, whereas without a magnetic field the kinetics in an ensemble of free carriers is determined by electrons with small effective masses, at $H \parallel [100]$ the translational motion of all the electrons is described by one heavy mass $1.43m_0$.

Owing to the large mass, the velocity $v = (2kT/m^*)^{1/2}$ of the thermal electrons turns out at helium temperatures to be of the order of the sound velocity s (the velocity of longitudinal sound in the [100] direction is $s_l = 4.92 \times 10^5$ cm/sec and that of transverse sound is $s_{tr} = 3.54 \times 10^5$ cm/sec). Yet it is known that phonon emission is difficult at $2s > v > s$ and entirely impossible at $s > v$.^[18] These limitations remain valid also in the presence of a magnetic field—see the Appendix. Therefore establishment of the final equilibrium between the thermal electrons and the lattice, and of the probability of the phonon scattering of the equilibrium part of the electron gas, should change strongly with temperature.

If the electrons and the scattering centers are in thermal equilibrium, then the resonance manifests itself in scattering via an increase of the collision frequency.^[2] Under non-equilibrium conditions the resonance can appear also in different ways. First, if the electron-electron collisions turn out to be more probable than phonon emission during the last stage of the cooling of the thermal electrons, then resonance scattering, by changing the number of thermal electrons, changes also the energy influx into the electron system.^[19] The effective temperature of the electron gas is changed as a result. A similar effect is observed also in measurements of the photomagnetic emf in InSb.^[8,13]

Second, the very process of cooling of thermal electrons by phonons causes a singularity to appear in their

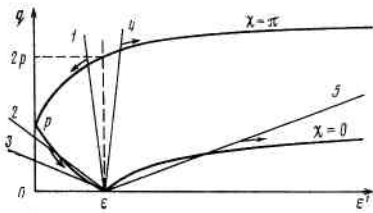


FIG. 9. Graphic solution of Eqs. (11) and (13). The lines 1 and 4 correspond to the inequality $\varepsilon > 2m^*s^2$, line 2 to the inequalities $2m^*s^2 > \varepsilon > m^*s^2/2$, and lines 3 and 5 to the condition $\varepsilon < m^*s^2/2$.

distribution function at $\varepsilon = \mathcal{N} \hbar \Omega$.^[20, 21] At such a distribution function, inelastic scattering with transfer of the characteristic energy ε should also lead to oscillations. These oscillations, however, are determined by the thermal electrons, a fact in poor agreement with the observed temperature dependences.

Third, in crossed electric and magnetic fields, the shift of the center of the electron orbit changes the potential energy of the electron. In the simplest case, when an electron temperature T_e can be introduced, its deviation from the effective neutral-acceptor temperature $kT_a = \mathcal{E} / \ln[(N_A - N^*)/N^*]$ (N^* is the number of excited acceptors) suffices already to produce, as a result of inelastic scattering, an electron flux directed opposite to the forces of the electric field. Effects of this type are known to occur in semiconductors.^[22, 23] A feature of this mechanism in comparison with two preceding ones is that it singles out the transverse conductivity. We recall in this connection that in our experiments the kinetic characteristics, determined by the conductivity in parallel electric and magnetic fields, oscillate relatively weakly (the potential difference $U^{(1)}$ in longitudinal (Sec. 4) and the longitudinal magnetoresistance (Sec. 7)).

Fourth and finally, when the diffusion current and the field current that cancel them are produced by different groups of carriers, the off-diagonal components of the conductivity tensor can lead to overcompensation that in principle can cause even a reversal of the sign of the field E_{GH} ,^[24, 14] let alone the sign of the oscillations. We note in this connection that the relation between the quantities n_1 , n_2 , and n_3 changes both with temperature, on which the rate of recombination and the value of n_3 depend, and with the illumination intensity: $n_{1,2} \propto I$ and $n_3 \propto I^{1/2}$ (assuming quadratic recombination). It is possible also that the ratio n_2/n_3 oscillates with the field, since resonant scattering changes the electron energy distribution. We note that experiment in very fact indicates that the concentrations n_i are the most important parameters of the problem (see Secs. 2 and 6).

The final answer to the question of which of the foregoing effects are the most significant and what causes the large magnitude of the oscillations and their inversions can be provided probably only by calculation. The model-dependent arguments of this section should be regarded only as an attempt to formulate more or less clearly the conditions of the problem.

The authors thank I. B. Levinson and É. I. Rashba for useful discussions and V. S. Zlobin and I. P. Luneva for help in preparing the samples.

APPENDIX

The character of the restrictions imposed on the electron-phonon scattering by the conservation laws was graphically illustrated in^[18]. Writing the conservation laws in the form

$$q = (2m^*)^{1/2} [\varepsilon + \varepsilon' - 2(\varepsilon\varepsilon')^{1/2} \cos \chi]^{1/2}, \quad (10)$$

$$\varepsilon' = \varepsilon \pm sq \quad (11)$$

(q is the phonon momentum; χ is the scattering angle and can take on all values from 0 to π in the absence of a magnetic field; ε and ε' are the energies of the electron before and after scattering; the dispersion law is quadratic and isotropic: $\varepsilon = p^2/2m^*$), we can construct the function $\varepsilon'(q)$ on the basis of Eq. (10), with ε and χ regarded as parameters. Figure 9 shows the curves for $\chi = 0$ and $\chi = \pi$; the curves corresponding to other values of χ fill the entire band between them. The solutions of the system (10) and (11) are obtained on the segments of the straight lines (11) located inside this band. Lines 1–3 correspond to phonon emission, lines 4 and 5 to absorption; the relative slope of the line, i. e., the relative locations of the line and of the curves with $\chi = 0$ and π , depends on the initial energy.

In a magnetic field, χ can assume only the values 0 and π , and all that is left of the band are the bounding curves. Equation (11) is transformed into

$$\varepsilon' = \varepsilon \pm s(q^2 + q_{\perp}^2)^{1/2}. \quad (12)$$

q is now the phonon momentum component along the magnetic field, and q_{\perp} is the momentum component perpendicular to this field, to which the momentum-conservation laws do not apply; $q_{\perp} \lesssim \hbar/r$, where $r = (2\hbar c/eH)^{1/2}$ is the so-called magnetic length. All the solutions of the system (10) and (12) lie on the $\chi = 0$ and $\chi = \pi$, and vary from the point of intersection with the line (11) in the direction indicated by the arrows.

Thus, all the limitations that apply without a magnetic field remain in force: at $v < 2s$ it becomes impossible to emit a phonon with change of the direction of the translation motion (line 2), at $v < s$ phonon emission is entirely impossible (line 3) and the absorption acquires a threshold on the side of low phonon energies: $(qs)_{\min} = 2m^*s^2 - 2(2m^*s^2\varepsilon)^{1/2}$ (line 5). In particular, at $\varepsilon < \varepsilon_0 = (6 - 4\sqrt{2})m^*s^2$ the energy of the absorbed phonon must be larger than the initial electron energy; this means that at $kT < \varepsilon_0$ the equilibrium electrons cease to absorb the equilibrium phonons.

¹V. F. Gantmakher and V. N. Zverev, Zh. Eksp. Teor. Fiz. 69, 695 (1975) [Sov. Phys. JETP 42, 352 (1976)].

²V. L. Gurevich and Yu. A. Firsov, Zh. Eksp. Teor. Fiz. 40, 199 (1961) [Sov. Phys. JETP 13, 137 (1961)].

³R. V. Parfen'ev, G. I. Kharus, I. M. Tsidil'kovskii, and S. S. Shalyt, Usp. Fiz. Nauk 112, 3 (1974) [Sov. Phys. Usp. 17, 1 (1974)].

- ⁴L. Eaves, R. A. Stradling, S. Askenazy, R. Barbaste, G. Garrere, J. Leotin, J. C. Portal, and J. P. Umet, *J. Phys. C* **7**, 1999 (1974).
- ⁵R. L. Jones and P. Fisher, *J. Phys. Chem. Solids* **26**, 1125 (1965).
- ⁶H. P. Soepangkat and P. Fisher, *Phys. Rev. B* **8**, 870 (1973).
- ⁷S. S. Shalyt, in: *Poluprovodniki v nauke i tehnike (Semiconductors in Science and Engineering)* **1**, AN SSSR, 1957, p. 43.
- ⁸R. V. Parfen'ev, I. I. Farbshtein, and S. S. Shalyt, *Zh. Eksp. Teor. Fiz.* **53**, 1571 (1967) [*Sov. Phys. JETP* **26**, 906 (1968)].
- ⁹G. Ascarelli and S. Rodriguez, *Phys. Rev.* **124**, 1321 (1961).
- ¹⁰R. A. Brown and S. Rodriguez, *Phys. Rev.* **153**, 890 (1967).
- ¹¹K. Colbow, *Can. J. Phys.* **41**, 1801 (1963).
- ¹²B. I. Shklovskii, *Fiz. Tekh. Poluprovodn.* **6**, 1197 (1972) [*Sov. Phys. Semicond.* **6**, 1053 (1973)].
- ¹³R. I. Lyagushchenko, R. V. Parfen'ev, I. I. Farbshtein, S. S. Shalyt, and I. N. Yassievich, *Fiz. Tverd. Tela* **10**, 2241 (1968) [*Sov. Phys. Solid State* **10**, 1764 (1969)].
- ¹⁴R. I. Lyagushchenko and I. N. Yassievich, *Fiz. Tverd. Tela* **9**, 3547 (1967) [*Sov. Phys. Solid State* **9**, 2794 (1968)]; *Zh. Eksp. Teor. Fiz.* **56**, 1432 (1969) [*Sov. Phys. JETP* **29**, 767 (1969)].
- ¹⁵I. K. Kikoin and S. D. Lasarev, *J. Phys. Chem. Solids* **28**, 1237 (1967).
- ¹⁶Sh. M. Kogan, V. D. Shadrin, and A. Ya. Shul'man, *Zh. Eksp. Teor. Fiz.* **68**, 1377 (1975) [*Sov. Phys. JETP* **41**, 686 (1975)].
- ¹⁷J. C. Slater, *Insulators, Semiconductors and Metals*, McGraw-Hill, 1967 [Russ. Transl., Mir, 1969].
- ¹⁸P. A. Kazlauskas and I. B. Levinson, *Lit. Fiz. Sb.* **6**, 33 (1966).
- ¹⁹R. V. Pomortsev and G. I. Kharus, *Fiz. Tverd. Tela* **9**, 1473, 2870 (1967) [*Sov. Phys. Solid State* **9**, 1150 (1967), 2256 (1968)].
- ²⁰E. Yamada and T. Kurosawa, *J. Phys. Soc. Japan* **34**, 603 (1973).
- ²¹E. Yamada, *Solid State Commun.* **13**, 503 (1973).
- ²²A. S. Aleksandrov, Yu. A. Bykovskii, V. F. Elesin, E. A. Protasov, and A. G. Podionov, *Zh. Eksp. Teor. Fiz.* **64**, 231 (1973) [*Sov. Phys. JETP* **37**, 120 (1973)].
- ²³V. I. Ryzhii, *Zh. Eksp. Teor. Fiz.* **64**, 643 (1973) [*Sov. Phys. JETP* **37**, 326 (1973)].
- ²⁴V. F. Elesin and Yu. A. Bykovskii, *Pis'ma Zh. Eksp. Teor. Fiz.* **6**, 497 (1967) [*JETP Lett.* **6**, 29 (1967)].

Translated by J. G. Adashko